Received: 3 March 2020 | Revised: 18 May 2020 | Accepted: 19 May 2020

DOI: 10.1002/er.5654

RESEARCH ARTICLE

INTERNATIONAL JOURNAL OF ENERGY RESEARCH WILEY

Neural network-based learning and estimation of battery state-of-charge: A comparison study between direct and indirect methodology

Wen Sun[1] | **Yicheng Qiu**[1] | **Li Sun**[1] | **Qingsong Hua**[2]

[1]Key Lab of Energy Thermal Conversion and Control of Ministry of Education, School of Energy and Environment, Southeast University, Nanjing, China

[2]Key Laboratory of Beam Technology of Ministry of Education, College of Nuclear Science and Technology, College of Nuclear Science and Technology, Beijing Normal University, Beijing, China

Correspondence
Li Sun, Key Lab of Energy Thermal Conversion and Control of Ministry of Education, School of Energy and Environment, Southeast University, Nanjing 210096, China.
Email: sunli12@seu.edu.cn

Qingsong Hua, College of Nuclear Science and Technology, Beijing Normal University, 100875, Beijing, China.
Email: 11112019039@bnu.edu.cn

Funding information
National Natural Science Foundation of China, Grant/Award Numbers: 51806034, 51936003; Natural Science Foundation of Jiangsu Province, China, Grant/Award Number: BK20170686

Summary

Faced with the ever-increasing urban environmental pollution, the electric vehicles (EVs) have received increasing attention in the automotive industry. Lithium-ion batteries, serving as electrochemical power storage, have been extensively used in EVs because of the lightweight, no local pollution and high power density. The increasing awareness on the safe operation and reliability of the battery requires an efficient battery management system (BMS), among the parameters monitored by which, state-of-charge (SOC) is critical in preventing overcharge, deep discharge, and irreversible damage. This article investigates the neural network (NN)-based modeling, learning, and estimation of SOC by comparing two different methodologies, that is, direct structure with SOC as network output and indirect structure with voltage as output. Firstly, the nonlinear autoregressive exogenous neural network (NARX-NN) is introduced, in which SOC is directly deemed as an NN output for learning and estimation. Secondly, a radial basis function (RBF)-based NN with unscented Kalman filter (RBFNN-UKF) is proposed, in which the terminal voltage is used as output. Instead, SOC is deemed as an internal state which would be estimated indirectly based on the feedback error of voltage. Experimental results demonstrate that both estimators can achieve accurate SOC estimation for regular cases, in spite of the inaccurate initial conditions. However, the direct NN structure is revealed as not capable of dealing with the cases with sensor bias, which, however, can be well accommodated in the indirect structure by extending the sensor bias as an augmented state. Benefiting from the uncertainty augmentation and feedback compensation, the indirect RBFNN-UKF shows superiority over the direct estimation in the practical experiments, depicting a promising prospect in the future onboard EV-BMS application.

KEYWORDS

lithium-ion battery, NARX neural network, sensor bias, state-of-charge (SOC), unscented kalman filter (UKF)

1 | INTRODUCTION

1.1 | Background

The last decade witnessed the unstoppable trend of the automotive industry upgrading from the internal combustion engine vehicle to the electric vehicle (EV), because of the rapid development and continuous cost reduction of the lithium-ion battery.[1] The lithium-ion battery stands out due to the multiple features such as lightweight, low self-discharge, fast charging, long lifetime and high power density[2-4] compared with other rechargeable batteries, thus being the primary choice for the electricity storage.

An efficient battery management system (BMS) is necessary to ensure the reliability and safety of the battery, which should efficiently monitor the charged state,[5] state of health (SOH)[6] and internal temperature.[7] Among the parameters monitored by BMS, the state-of-charge (SOC), defined as the ratio of the available capacity to the full capacity,[8] is a critical indicator of the remaining battery power and directly reflects the operational condition.[9] Overcharge or over discharge of the battery can sometimes be attributed to the inaccurate SOC estimation, which may even cause irreversible damage to the battery.[10] In contrast, an accurate estimation of SOC offers the advantages including enhancing the battery safety, making the best of the battery potential, and improving the efficiency.[11]

However, the battery SOC is unmeasurable by existing sensors, but can be estimated via other measurable signals. The high nonlinearity of lithium-ion battery system makes the SOC estimator design a quite cumbersome task, to which the researches we turn next.

1.2 | State-of-the-art

Commonly numerous research approaches existing in evaluating the battery SOC cover distinct algorithm, models, and neural networks (NNs).

The commonly used ampere-hour counting algorithm characterized by the most simplicity and directness,[12] is known to have issues with the initial SOC value and accurate current measurements.[13]Due to the feature associated with an open-loop algorithm, however, cumulative error effect occurring in calculating SOC value can be attributed to the uncertain interference such as temperature and current measurement deviation.[14]

Taking the open circuit voltage (OCV) method[15] into account to estimate SOC is feasible only in the case where the battery has been relaxed for sufficient time to reach a stable state, this is because the electrochemical potential is in close connection with the residual active substance in the electrodes.[16] In line with the relation curve between the OCV and SOC, SOC corresponding to the appointed voltage can be derived by measuring the OCV. Since the load is required to be discharged from the electric circuit, however, this method fails in practical applications where SOC should be estimated online. Moreover, equilibrium requires the battery quitely placing for more than 2 hours,[5] resulting in a serious waste of time. The approach of building an OCV relaxation model given in Reference 17 has been used to reduce the relaxation time.

Machine learning has been deeply entrenched in industrial control.[18-21] Therein, NN, developed as SOC estimators, have been studied extensively in the literature, including back-propagation neural networks (BP-NN),[22,23] radial basis function neural networks (RBFNN).[24,25] In the NN model for SOC estimation, a large mass of known input data and expected output data obtained from the battery charging and discharging experiments is required to train the network, thereby self-learning the network parameters and extracting the fitting relationship. Instead, a mathematical model of the system and the complex reaction mechanism inside the battery need not to be considered. Moreover, benefiting from the extensive applications in any type of battery SOC estimation and ability to self-learn the network parameters, NN method offers competitive performance in solving nonlinear problems for SOC estimation.

Kalman filter (KF) algorithm has been validated as a formidable tool for SOC estimation due to its closed-loop feature and ability to easily deal with uncertainties. Extended Kalman filter (EKF)[26,27] is often employed to deal with nonlinear estimation problems, as well as unscented Kalman filter (UKF).[28,29] In References 24 and 30, EKF has been implemented in conjunction with NN to estimate SOC. Based on RC model, EKF and UKF developed in Reference 31 are proposed to realize effective SOC estimation, respectively. Moreover, the ampere-hour algorithm has been carried out in conjunction with UKF to estimate SOC.[32]

1.3 | Current limitations and proposed innovations

The aforementioned SOC estimation approaches including ampere-hour counting algorithm, OCV method are commonly known to have their limitations in terms of unknown initial SOC value, impossibility of SOC estimation online, and the existing NN models have issues with data over fitting, low convergence, and are easy to trapped in local optimum.[33] The nonlinear autoregressive exogenous neural network (NARX-NN) with external input possesses the ability to effectively address time series

problem and offers a better performance in convergence speed and estimation accuracy, which enhances its superiority for the estimation of SOC compared with the BP-NN and RBFNN. A NARX-NN is proposed where the battery current and terminal voltage are denoted as input and SOC is taken as output to accurately estimate the battery SOC. Since this NARX-NN maps battery measurements including current and terminal voltage directly to SOC, this proposed approach is called the direct structure in this article.

Kalman filter (KF) algorithm featured by the feedback plays a highly significant role in a strong suppression of system noise. Compared with other approaches, KF offers competitive performance in estimating SOC in case that the batteries suffer from unstable dynamics during the process of repeated acceleration and deceleration of power vehicles. Consequently, KF based on a discrete linear state-space model has been spotlighted for use in battery SOC estimation. To accommodate the nonlinearity, UKF based on RBFNN model is proposed (ie, original RBFNN-UKF model), where SOC is defined as the internal state and can be estimated indirectly based on the voltage (ie, output variable) error. Therefore, this proposed approach is called the indirect structure in this article. The robustness of UKF employedin[32] for SOC estimation, however, is poor in case of model in accuracy. The indirect structure proposed in this article seeks to apply UKF to the RBFNN model (ie, original RBFNN-UKF) to estimate SOC with high precision and fast convergence.

It is widely acknowledged that the estimation accuracy inevitably deteriorates in case that sensor biases exist in the battery measurements like current and terminal voltage, which may be attributed to sensor aging or calibration errors. The proposed direct NN structure is revealed as not capable of dealing with such cases with sensor bias, which, however, can be well accommodated in the proposed indirect structure. In the RC model given in Reference 31, EKF and UKF using augmented model are redesigned to realize the precise SOC evaluation in the presence of sensor biases. A new method for diagnosing current sensor bias (ie, extended RBFNN-UKF) is proposed here by extending an augmented state into the original indirect structure to accurately estimate SOC together with unknown current sensor bias. Additionally, experimental comparison results of the designed original RBFNN-UKF and extended RBFNN-UKF for SOC estimation in the presence of current sensor bias are carried out.

The motivation of incorporating the extended state estimation method into NN framework lies in its recent success in various energy systems, such as conventional power plant control,[34] fuel cell uncertainty estimation[35] and temperature control.[36] The combination will exploit the merits of both methodologies for accurate dynamic modeling and uncertainty compensation. The rest of the article is structured as follows. The direct estimation method using NARX-NN is developed in Section 2. The closed-loop NN framework in which the extended state based UKF estimation can be equipped is formulated in Section 3. Section 4 reveals the experimental results and Section 5 draws the conclusion.

2 | DIRECT ESTIMATION BASED ON NARX-NN

2.1 | NARX-NN based direct modeling

In the prediction for time-series data, a NARX-NN, consisting of three layers-input layer, hidden layer, and output layer, is a nonlinear autoregressive model which has exogenous inputs. NARX-NN is featured by the input layer, which does not only contain the exogenous input series, but also contains the past values of the same-series output. Among the parameters in this network, the input delay, output backward time-delay order and the number of hidden layer neurons remarkably impact the network performance. Due to the time delay and backward in the structure of the NN, NARX-NN possesses memory and association function for the historical information and is powerfully adaptable for time varying regularity of time sequences with multiple inputs and multiple outputs. Figure 1 shows the structure of NARX-NN for direct modeling.

2.2 | Establishment, identification, and testing for the direct NN estimator

Due to the fact that the battery SOC is closely associated with the current and terminal voltage, the input variables fed into the proposed NARX-NN are deemed as the battery current and terminal voltage, SOC at the same sampling time obtained from the battery charging and discharging experiment is considered as the only output of the network, according to which a three-layer NARX-NN is constructed ultimately and programmed on MATLAB. The mathematical expression of NARX-NN with two-dimensional input and one-dimensional output is represented by,

$$y(n+1)=f_0\left[b_0+\sum_{h=1}^{N}w_{h_0}f_h\left(b_h+\sum_{k=1}^{2}\sum_{i_k=0}^{d_{uk}}w_{i_k h}u_k(n-i_k)+\sum_{j=0}^{d_y}w_{jh}y(n-j)\right)\right] \quad (1)$$

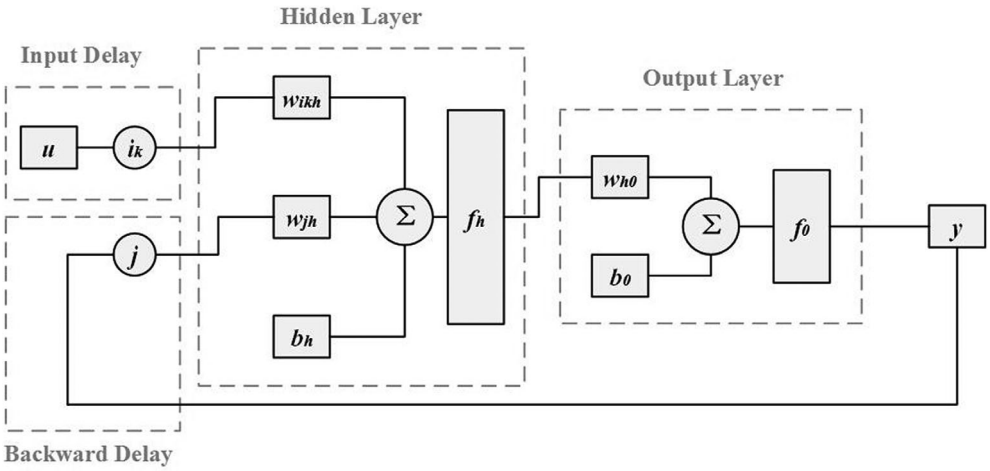

FIGURE 1 Structure of NARX-NN for direct modeling. NARX-NN, nonlinear autoregressive exogenousneural network

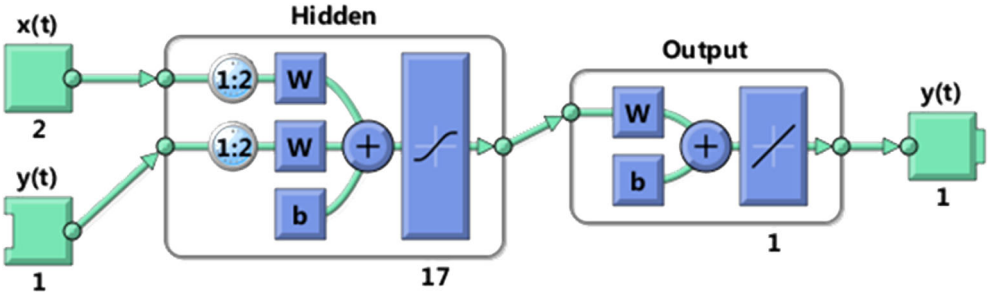

FIGURE 2 Open-loop training mode of the direct NARX-NN. NARX-NN, nonlinear autoregressive exogenousneural network [Colour figure can be viewed at wileyonlinelibrary.com]

where the nonlinear functions f_0 and f_h are defined by the output layer and hidden layer, respectively. $u(.)$ and $y(.)$ are used to characterize the input and output of the NN, respectively. i_k represents the input delay and j is the output backward delay. The weights between two layers are represented by $w_{i_k h}$, w_{h_0}, w_{jh}, respectively. The bias weights b_0 and b_h are added to the matrix multiplication to strengthen the NARX-NN flexibility.

Benefiting from self-learning the network parameters, identification for NARX-NN is determined by the training phase of NARX-NN, the open-loop mode (where the target values take place of the predicted values and are, then, backward to the input side with time-delay, so as to improve the network training accuracy) tends to be adopted to train the network for SOC estimation. Consequently, the training set data including input and expected output data can be fed into the network with the open-loop mode, which has been programmed on MATLAB. NARX-NN with optimal parameters will be determined by the training set data. Figure 2 shows the open-loop training mode of the direct NARX-NN, where 17 neurons are set in the hidden layer, and 1:2 is defined as the input and output time-delay order.

Independent test set data is then utilized during the test phase of NARX-NN to validate the proposed direct NN estimator's ability to perform well in SOC estimation. Since the target values are unknown during testing, open-loop training mode of NARX-NN is transformed into a closed-loop mode, where the predicted SOC values are backward to the input with time-delay. The closed-loop testing mode of NARX-NN is shown in Figure 3, where the network parameters have been self-learned in the training phase.

3 | INDIRECT ESTIMATION BASED ON RBFNN-UKF

3.1 | RBFNN based modeling

RBFNN is a forward NN that possesses strong nonlinear fitting ability that can approximate arbitrary nonlinear function with desired accuracy, which is similarly composed of three layers. The structure of RBFNN for indirect modeling is demonstrated in Figure 4, where the optimal weight vector and bias weight between the hidden layer and output layer are determined during the training phase, as well as the number of hidden layer neurons. The activation function of hidden layer neurons often employs the RBF (typically is the Gaussian function), the center and width of which are determined during the same network training process. RBFNN trained by the known input and output data then serves as the appropriate model in the UKF.

In the indirect modeling, the input vector and output vector fed into the RNFNN are defined as $X = [x_1, x_2, x_3]^T$ and y,

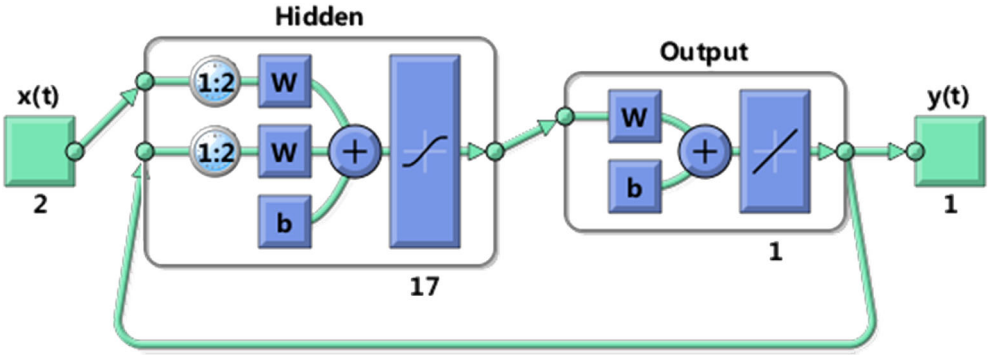

FIGURE 3 Closed-loop testing mode of the direct NARX-NN. NARX-NN, nonlinear autoregressive exogenousneural network [Colour figure can be viewed at wileyonlinelibrary.com]

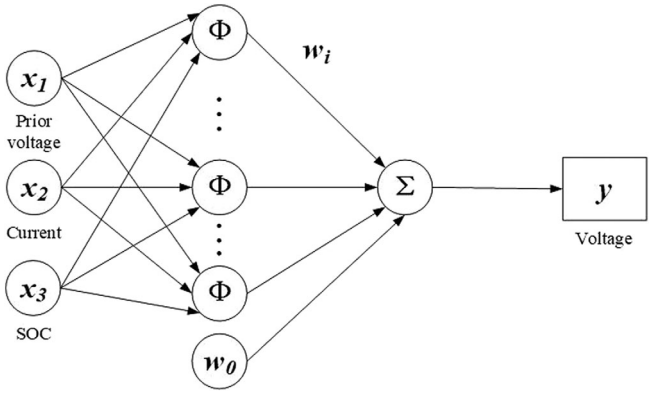

FIGURE 4 Structure of RBFNN for indirect modelling. RBFNN, radial basis function neural network

respectively. The activation function (typically is the Gaussian function) in the hidden layer can be expressed by φ,

$$\varphi(X) = \exp\left(-\frac{X - c_i^2}{\sigma^2}\right) \tag{2}$$

where $c_i = [c_{i1}, c_{i2}, c_{i3}]^T$ and σ represent the center and width of ith hidden layer neuron, respectively, which will be defined in the training phase. $\|.\|$ denotes Euclidean norm. The output of this network is calculated by the bias weight and weighted Gaussian function,

$$F(X) = w_0 + \sum_{i=1}^{M} w_i \varphi(X) \tag{3}$$

where F is the nonlinear function from the input to the output defined by the trained RNFNN. M denotes the number of hidden layer neuron. w_0 set to increase the network flexibility is the bias weight, $w_i = [w_1, w_2, ..., w_n]^T$ is considered as the weight vector, indicating the mapping relationship from the hidden layer to the output layer. By contrast, the input vector is directly mapped to the hidden layer.

3.2 | Establishment, identification, and validation for RBFNN

The control differential equation of first order between the battery current and terminal voltage is developed in the commonly employed RC model to estimate SOC. Therefore, it is theoretically demonstrated that deeming the terminal voltage as a nonlinear function of SOC, current and prior terminal voltage is reasonable in the discrete model.[24,37] In the RBFNN model established in this article, the battery SOC, current and prior terminal voltage are consequently regarded as the inputs, the terminal voltage is the output, which has been demonstrated in Figure 4. Hence, the RBFNN for estimating the terminal voltage is constructed ultimately, where SOC is treated as one of the input variables.

Similarly, identification for RBFNN is determined by the training phase. The structure of trained RBFNN is shown in Figure 5, where 73 neurons in the hidden layer with $\sigma = 0.8326$ have been defined. Since an accurate model that describes the battery dynamics is indispensable for state estimation, essential validation for the established indirect model accuracy should be exercised on the RBFNN. The sampling data obtained from the battery charging and discharging experiment is then adopted in the test for validation. It follows from Figure 6 that the disparity between the RBFNN output (ie, the predicted terminal voltage) and the actual value is small enough to verifies the accuracy and good performance of the established RBFNN model. Consequently, the optimal parameters such as center vector, base width and weight vector have then been defined and the trained RBFNN model is then fed into the UKF to estimate SOC.

3.3 | Unscented Kalman filter

Unscented Kalman filter is extensively applied to nonlinear control applications and deal with state estimation problems, the core of which is a kind of nonlinear transformation to deal with the nonlinear propagation of mean value and

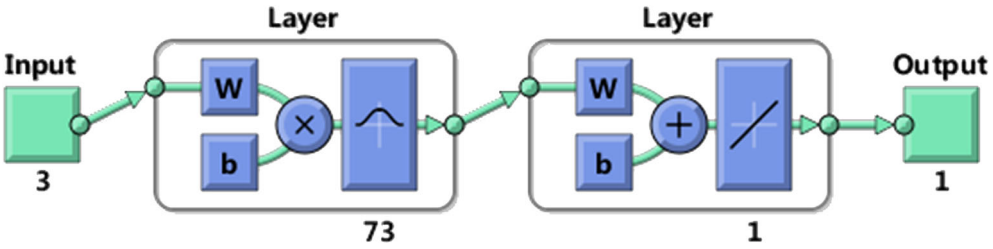

FIGURE 5 Structure of trained RBFNN. RBFNN, radial basis function neural network [Colour figure can be viewed at wileyonlinelibrary.com]

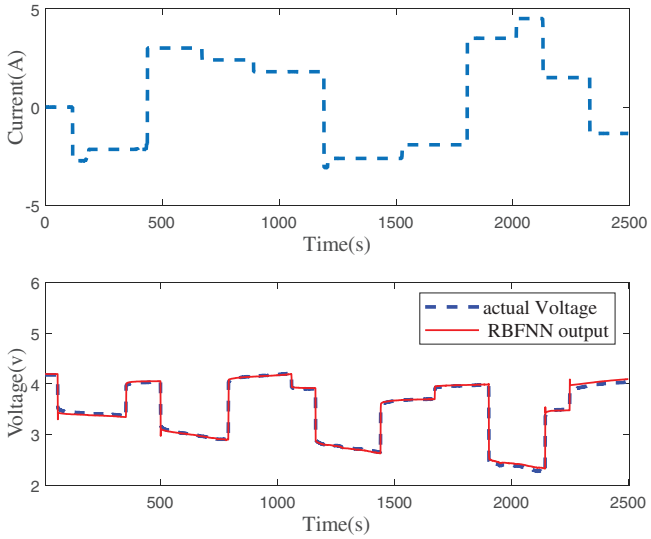

FIGURE 6 Experimental data and results for validation [Colour figure can be viewed at wileyonlinelibrary.com]

covariance. The distribution of the input states is represented by the sigma points, and then these sigma points are subject to the nonlinear transformation. Hence, sigma points and covariance functioned by the nonlinear transformation are finally derived. This nonlinear transformation (ie, unscented transformation) algorithm is given as follows:

Define a matrix χ of $2n + 1$ sigma vectors on the basis of mean value and covariance of random vector x,

$$\begin{aligned}\chi_0 &= \hat{x}\\ \chi_i &= \hat{x} + \left(\sqrt{(n+\lambda)P_x}\right)_i \quad i = 1,\ldots,n\\ \chi_i &= \hat{x} - \left(\sqrt{(n+\lambda)P_x}\right)_{i-n} \quad i = n+1,\ldots,2n\end{aligned} \tag{4}$$

Intermediate parameter Y_i can be derived by the propagated sigma vectors,

$$Y_i = g(\chi_i) \quad i = 0,\ldots,2n \tag{5}$$

The mean value $\hat{y}$ and covariance P_y of y are calculated by the function of the sigma points functioned by the nonlinear transformation and the weighted coefficient $W_i^{(m)}$, $W_i^{(c)}$.

$$\begin{aligned}\hat{y} &\approx \sum_{i=0}^{2n} W_i^{(m)} Y_i\\ P_y &\approx \sum_{i=0}^{2n} W_i^{(c)} (Y_i - \hat{y})(Y_i - \hat{y})^T\end{aligned} \tag{6}$$

$$\begin{aligned}W_0^{(m)} &= \lambda/(n+\lambda)\\ W_0^{(c)} &= \lambda/(n+\lambda) + (1 - \alpha^2 + \beta)\\ W_i^{(m)} &= W_i^{(c)} = 1/\{2(n+\lambda)\} \quad i = 1,\ldots,2n\end{aligned} \tag{7}$$

where scaling parameter $\lambda = \alpha^2(L + \kappa) - n$ is set by the defined α, κ, and n. Parameters such as α, β, κ required to be defined according to their features. The distribution of sigma points is determined by parameter α, typically set between le^{-4} and 1. Defined $\kappa = 0/3 - n$ is a secondary scaling parameter. Parameter β affecting the state distribution is typically set to 2for the optimal Gaussian distribution. The core algorithm of UKF has been demonstrated above. Meanwhile, state-space model for UKF is discretized as follows,

$$\begin{aligned}x_{k+1} &= f(x_k, u_k) + w_k\\ y_k &= h(x_k, u_k) + \nu_k\end{aligned} \tag{8}$$

where x_k, u_k, y_k are considered as the state, input and output vectors, respectively. $f(.)$ and $h(.)$ are used to present the nonlinear functions approximated by training the RBFNN. Measurement noise ν_k is added to the observation output and process noise ν_k denotes some stochastic unmodeled dynamics. Q_k and R_k are accordingly given by

$$\begin{aligned}Q_k &= E\left[w_k\, w_k{}^T\right]\\ R_K &= E\left[\nu_k\, \nu_k{}^T\right]\end{aligned} \tag{9}$$

UKF algorithm equations for SOC estimation are given as follows:

State variables and covariance initialization:

$$\begin{aligned}\hat{x}_0 &= E[x_0]\\ P_0 &= E\left[(x_0 - \hat{x}_0)(x_0 - \hat{x}_0)^T\right]\end{aligned} \tag{10}$$

Calculate sigma points through unscented transformation, then one-step prediction of the state variables

through the state-space equation and covariance of state variables are obtained:

$$\begin{aligned}
&\chi_{k-1}^{0} = \hat{x}_{k-1} \qquad i=0\\
&\chi_{k-1}^{i} = \hat{x}_{k-1} + \left(\sqrt{(n+\lambda)P_{k-1}}\right)_i \quad i=1,...,n\\
&\chi_{k-1}^{i} = \hat{x}_{k-1} - \left(\sqrt{(n+\lambda)P_{k-1}}\right)_{i-n} \quad i=n+1,...,2n\\
&\chi_{k|k-1}^{i} = f\left(\chi_{k-1}^{i}, u_{k-1}\right)\\
&\hat{x}_{k|k-1} = \sum_{i=0}^{2n} W_i^{(m)} \chi_{k|k-1}^{i}\\
&P_{x,k|k-1} = \sum_{i=0}^{2n} W_i^{(c)} \left[\chi_{k|k-1}^{i} - \hat{x}_{k|k-1}\right]\left[\chi_{k|k-1}^{i} - \hat{x}_{k|k-1}\right]^T + Q_k
\end{aligned} \tag{11}$$

Measurement update equations:

$$\begin{aligned}
y_{k|k-1}^{i} &= h\left(\chi_{k|k-1}^{i}, u_k\right)\\
\hat{y}_{k|k-1} &= \sum_{i=0}^{2n} W_i^{(m)} y_{k|k-1}^{i}
\end{aligned} \tag{12}$$

Kalman gain, state variables and error covariance update equations:

$$\begin{aligned}
P_{yy,k} &= \sum_{i=0}^{2n} W_i^{(c)} \left[y_{k|k-1}^{i} - \hat{y}_{k|k-1}\right]\left[y_{k|k-1}^{i} - \hat{y}_{k|k-1}\right]^T + R_k\\
P_{xy,k} &= \sum_{i=0}^{2n} W_i^{(c)} \left[\chi_{k|k-1}^{i} - \hat{x}_{k|k-1}\right]\left[y_{k|k-1}^{i} - \hat{y}_{k|k-1}\right]^T\\
K_k &= P_{xy,k} P_{yy,k}^{-1}\\
\hat{x}_{k|k} &= \hat{x}_{k|k-1} + K_k\left(y_k - \hat{y}_{k|k-1}\right)\\
P_{x,k|k} &= P_{x,k|k-1} - K_k P_{yy,k} K_k{}^T
\end{aligned} \tag{13}$$

Where the prior estimation of state variables and the error covariance are denoted by $\hat{x}_{k-1|k-1}$ and $P_{k-1|k-1}$, respectively. $\hat{x}_{k|k-1}$, $P_{k|k-1}$ are the posterior predicted value of the state variables and error covariance according to the function of the prior estimation, respectively. K_k is considered as the gain matrix which is updated over time. The nonlinear functions $f(.)$ and $h(.)$ are derived by the model fed into the UKF. Q_k and R_k are set by adding bias to the state and input measurements.

In the UKF algorithm for SOC estimation, after the initialization for the state variables, the algorithm predicts and updates the battery SOC within each sampling period. Meanwhile, the Kalman gain will be adjusted continuously and correct the estimated error by the feedback according to the error covariance. Time accumulation and the increase on the number of algorithm cycles enforce the estimated SOC approaching the true value. The UKF algorithm possesses the ability to rectify the estimated value based on the feedback error even if the initial value is not set equal to the true value. The estimated value can gradually approach the real value as the algorithm progresses. The flow chart of UKF to estimate SOC is shown in Figure 7.

3.4 | Design of indirect SOC estimator

The aforementioned RBFNN that defined by the training data is utilized as the nonlinear model for designing UKF. Several optimal parameters such as center vector, base width and weight vector have been defined before designing UKF as nonlinear SOC estimator, thereby the nonlinear state-space model in the UKF will be ultimately established and programmed on MATLAB.

SOC is defined as the ratio of the available capacity to the full capacity.[8]

$$s(t) = s(t_0) + \int_{t_0}^{t} \frac{\eta_i i(\tau)}{C_n} d\tau \tag{14}$$

where $s(t)$ and $s(t_0)$ represent the SOC and initial SOC value, respectively, C_n is considered as the nominal capacity. η_i is set to 1 which denotes Coulombic efficiency. The battery current $i(t)$ is positive/negative when the battery is in discharging/charging mode.

However, a discrete model employed in the UKF requires the aforementioned equation for defining SOC to be discretized. Given the sampling time Δt is short enough, the aforementioned equation can be alternatively represented by

$$s(k+1) = s(k) + \frac{\Delta t}{C_n} i(k) \tag{15}$$

In accordance with the defined input variables and output variable of RBFNN, the battery SOC and prior terminal voltage are, respectively, viewed as the first and second state vectors, the current and terminal voltage are, respectively, treated as the system input and output in UKF. The state vector and output vector of the system are defined as

$$\begin{aligned}
X_k &= \begin{bmatrix} x_1(k) \\ x_2(k) \end{bmatrix} = \begin{bmatrix} v(k-1) \\ s(k) \end{bmatrix}\\
X_{k+1} &= \begin{bmatrix} x_1(k+1) \\ x_2(k+1) \end{bmatrix} = \begin{bmatrix} v(k) \\ s(k+1) \end{bmatrix}\\
y_k &= v(k)
\end{aligned} \tag{16}$$

where the battery terminal voltage and SOC are denoted by v and s, respectively. In view of the aforementioned definition of SOC and state-space model for UKF, the state-space model can be accordingly written as

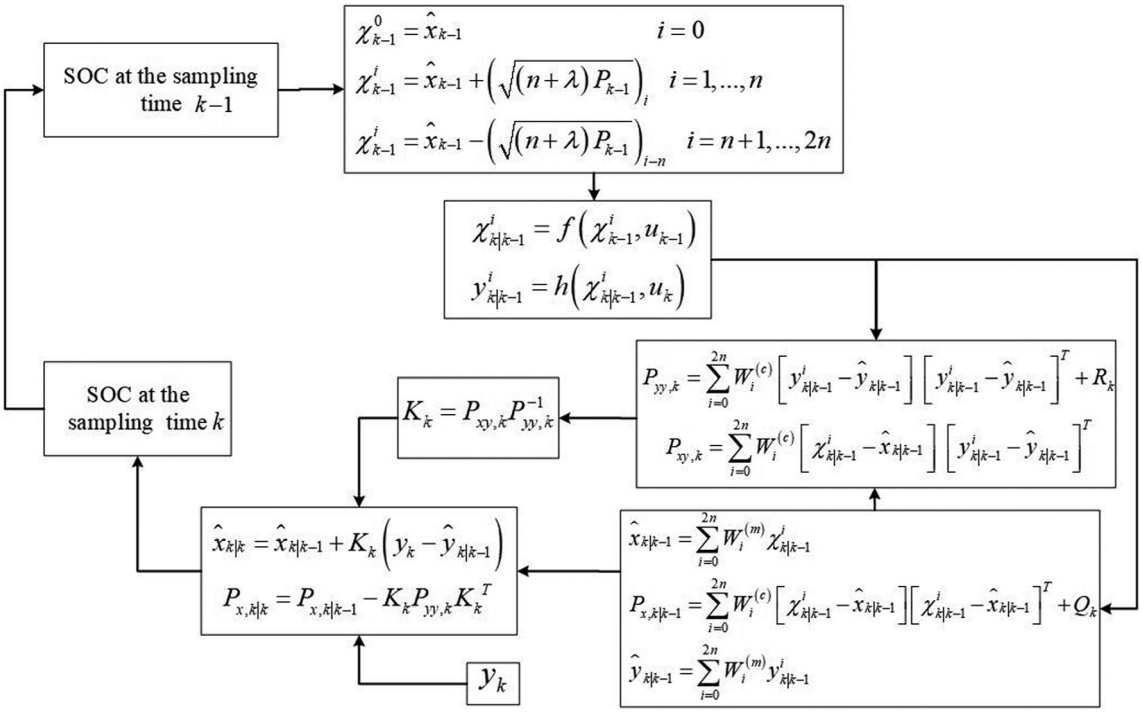

FIGURE 7 Flow chart of UKF to estimate SOC. NARX-NN, nonlinear autoregressive exogenousneural network; SOC, state-of-charge; UKF, unscented Kalman filter

$$X_{k+1} = \begin{bmatrix} x_1(k+1) \\ x_2(k+1) \end{bmatrix} = \begin{bmatrix} F([X_k; u_k]) \\ x_2(k) + \dfrac{\Delta t}{C_n} u_k \end{bmatrix} + \begin{bmatrix} w_1(k) \\ w_2(k) \end{bmatrix} \quad (17)$$
$$y_k = F([X_k; u_k]) + \nu(k)$$

where u_k is considered as the input in the UKF (ie, i_k). F is the nonlinear function approximated by the trained RBFNN.

3.5 | Design of indirect SOC estimator against sensor bias

It is worth noting that the estimation accuracy may significantly deteriorate in case that the battery measurements like current and terminal voltage are subject to the sensor bias. It is elaborated in Reference 38 that this issue can be addressed with hardware redundancy and analytical redundancy, respectively, utilizing redundant sensors and multiple models-based techniques. A new approach for sensor bias estimation together with SOC is proposed here by extending an augmented state into the original RBFNN-UKF, the efficacy of which will be proved feasible. For the case with unknown current sensor bias, denote the current sensor bias as the third internal state variable (ie, I_e) incorporated into the original two-state-space RBFNN-UKF. This bias is considered to be a constant value and initially unknown. Hence, the actual battery current can be represented by $i - I_e$. The state vector and output vector of the system are modified as follows,

$$X_k = \begin{bmatrix} x_1(k) \\ x_2(k) \\ x_3(k) \end{bmatrix} = \begin{bmatrix} v(k-1) \\ s(k) \\ b(k) \end{bmatrix}$$
$$X_{k+1} = \begin{bmatrix} x_1(k+1) \\ x_2(k+1) \\ x_3(k+1) \end{bmatrix} = \begin{bmatrix} v(k) \\ s(k+1) \\ b(k+1) \end{bmatrix} \quad (18)$$
$$y_k = v(k)$$

where the current sensor bias is represented by b_k. Since the bias is considered to be constant, $b_{k+1} = b_k$. As a result, the aforementioned state-space model now can be reformulated as

$$X_{k+1} = \begin{bmatrix} x_1(k+1) \\ x_2(k+1) \\ x_3(k+1) \end{bmatrix} = \begin{bmatrix} F([x_1(k); x_2(k); u_k - x_3(k)]) \\ x_2(k) + \dfrac{\Delta t}{C_n}(u_k - x_3(k)) \\ x_3(k) \end{bmatrix} + \begin{bmatrix} w_1(k) \\ w_2(k) \\ 0 \end{bmatrix}$$
$$y_{k+1} = F([x_1(k); x_2(k); u_k - x_3(k)]) + \nu(k) \quad (19)$$

Such a model is considered as the extended RBFNN-UKF model with three state variables, which can realize

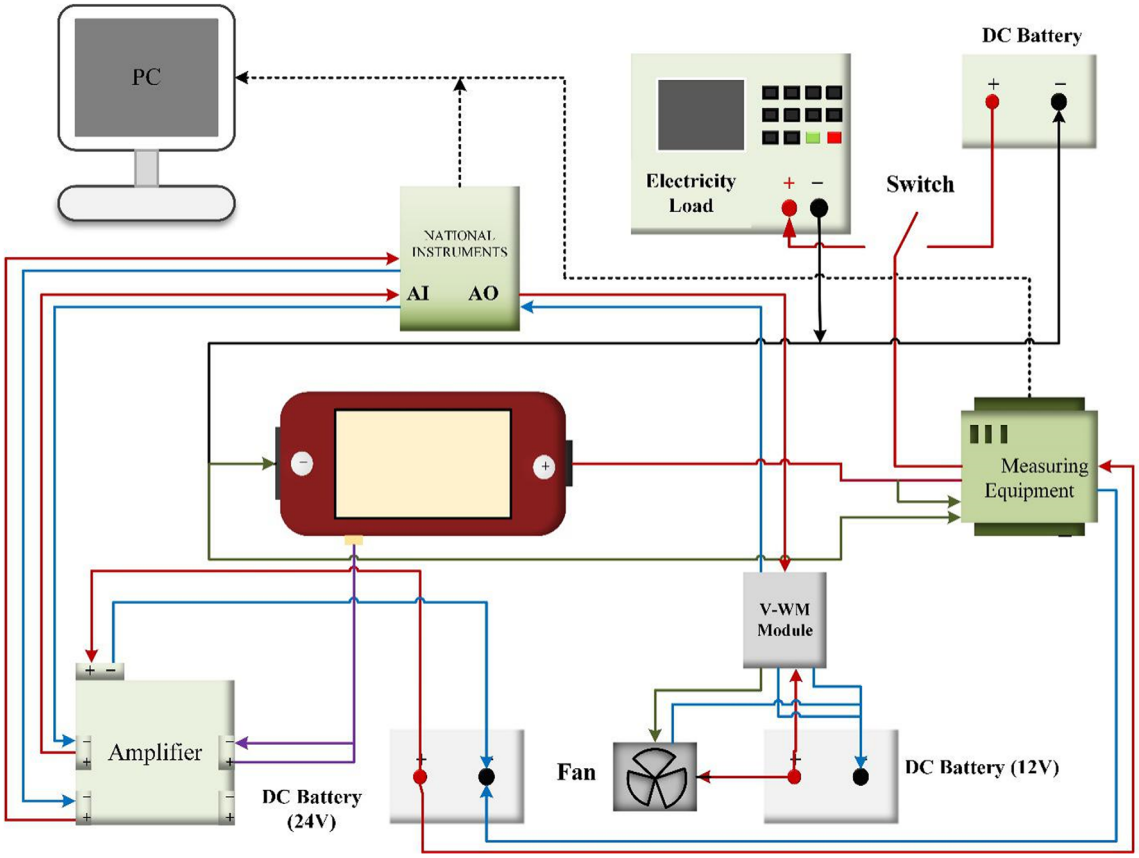

FIGURE 8 Schematic of the experimental setup [Colour figure can be viewed at wileyonlinelibrary.com]

simultaneous estimation for the current sensor bias and SOC, while the aforementioned two-state-space model is the original RBFNN-UKF model.

4 | EXPERIMENTAL RESULTS

4.1 | Experiment setup

The charging and discharging experiment is carried out on a 3450 mAh SANYO lithium-ion battery NCR 18650G. The proposed NNs and the UKF algorithm, are programmed based on MATLAB, which can be found in Supporting Information of this article. Figure 8 shows the schematic of the experimental setup, which consists of a computer, a controllable electronic load, a lithium-ion battery, an amplifier, a measuring equipment, and three DC batteries. For obtaining charging and discharging experimental data including the known battery current, terminal voltage, and SOC to train the NNs, a DC battery and an electronic load have been used to control the battery charging and discharging mode. During the process of the battery charging and discharging, which can be viewed on the computer monitor, variable pulse charging and discharging current was implemented on the battery, providing the NNs with a broad range of realistic conditions. The battery signals including the current, terminal voltage and temperature are transmitted to the computer via the RS-485 MODBUS-RTU protocol. The temperature data derived by the thermocouple is only used to monitor the battery to ensure its safety. The sampling period is set to 1 second for calculating SOC. To get the initial SOC value, the battery is charged to full state at the beginning, and then the SOC value of each step can be calculated using the ampere-hour counting algorithm defined in (15).

4.2 | Experiment results

The direct and indirect estimators are then tested on the experimental data. It is noted that experimental tests not only validate the outstanding performance of NARX-NN for SOC estimation, but also the robustness against different initial conditions. For different initial conditions: SOC(0) = 100%, SOC(0) = 53.08%, and SOC(0) = 22.20%, the curves of experimental results are shown in Figure 9, which demonstrates that the direct NARX-NN structure consistently achieves a high level of accuracy in estimating SOC from the initial moment and is insensitive to different initial conditions.

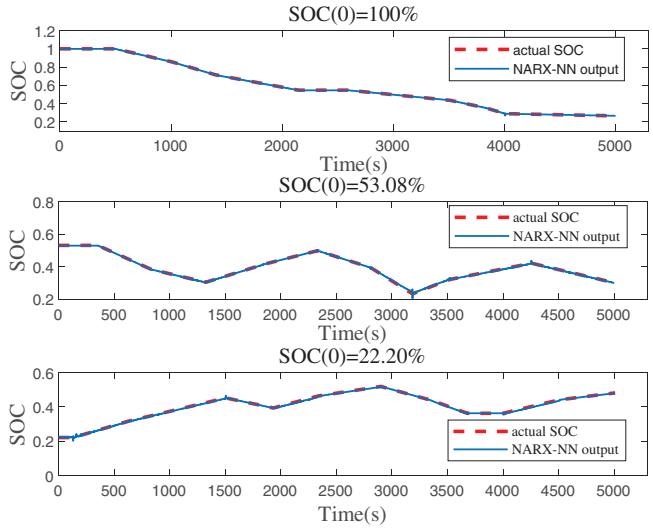

FIGURE 9 SOC estimation of the direct NARX-NN structure under different initial conditions. NARX-NN, nonlinear autoregressive exogenousneural network; SOC, state-of-charge [Colour figure can be viewed at wileyonlinelibrary.com]

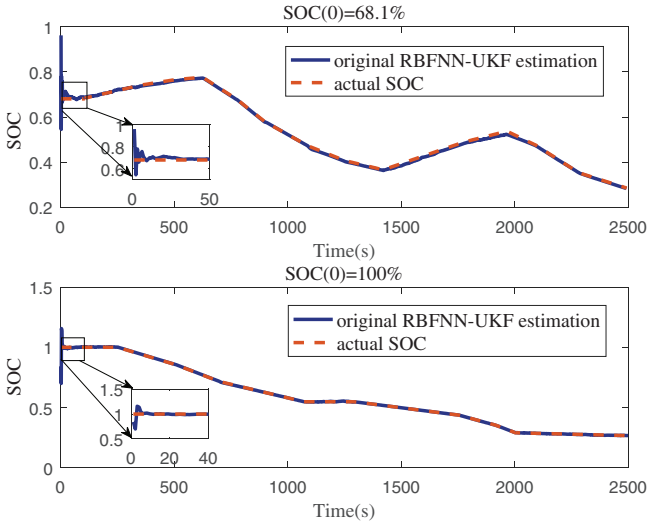

FIGURE 10 SOC estimation of original RBFNN-UKF structure under different initial conditions. RBFNN, radial basis function neural network; SOC, state-of-charge; UKF, unscented Kalman filter [Colour figure can be viewed at wileyonlinelibrary.com]

The other indirect structure based on RBFNN model (ie, original RBFNN-UKF) is implemented to estimate the same battery SOC. Experimental test is also conducted to validate the indirect estimator's ability to estimate SOC with high accuracy. Like the performance analysis of the NARX-NN, for different initial conditions: SOC(0) = 68.1%, SOC(0) = 100%, Figure 10 shows the true and estimated SOC values. It is obvious that for different initial conditions, SOC estimated by the indirect structure quickly converges to the true value in less than 50 seconds, which indicates that the proposed indirect estimator performs well in estimating SOC and is robust against different initial conditions. In general, experimental tests show that both direct and indirect estimators achieve similar overall accuracy, although the transient convergence of the direct NARX-NN is quicker than that of the indirect RBFNN-UKF estimator.

For the case with unknown current sensor bias, the direct NARX-NN structure is revealed as not capable of dealing with the cases with sensor bias and significantly deterioration on the SOC estimation accuracy is known to be inevitable. To this end, the extended RBFNN-UKF that extends the current sensor bias as the third internal state is designed to realize the simultaneous estimation of SOC and unknown current sensor bias. The current measurement is increased by 100 mA and this constant value is considered here as the current sensor bias. The curves of the true SOC value, SOC estimated by the original RBFNN-UKF model, and SOC estimated using the extended RBFNN-UKF model are compared in Figure 11. As illustrated in Figure 11, the SOC estimated using the

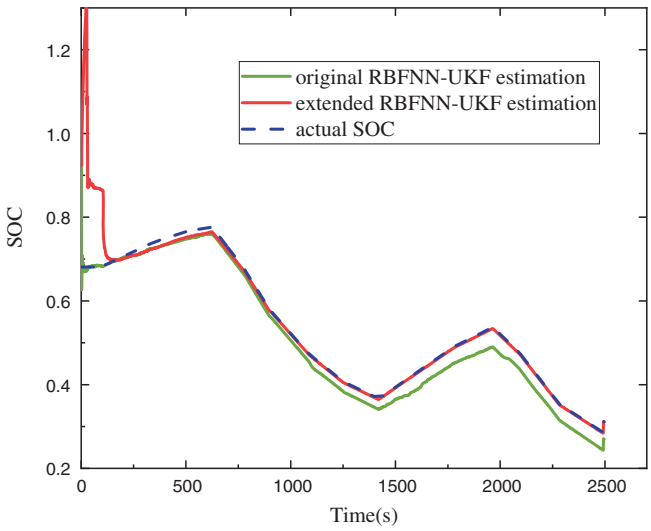

FIGURE 11 Curves of the true battery SOC, the SOC estimated by the original RBFNN-UKF model, and the SOC estimated using the extended RBFNN-UKF model. RBFNN, radial basis function neural network; SOC, state-of-charge; UKF, unscented Kalman filter [Colour figure can be viewed at wileyonlinelibrary.com]

extended RBFNN-UKF quickly converges to the real measurements, while the SOC estimated by the original RBFNN-UKF is always lower than that, and the error between the SOC estimated by the original RBFNN-UKF and true SOC seems to increase with the previous charging and discharging experimental period. On the whole, the disparity between the SOC estimated by the extended

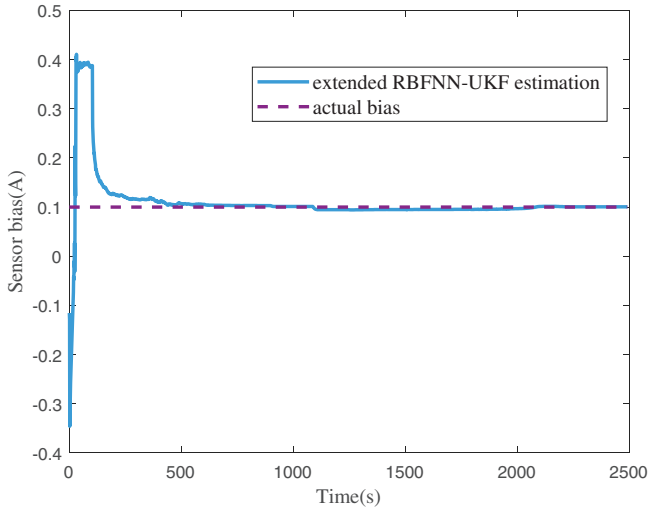

FIGURE 12 Current sensor bias estimated by the extended RBFNN-UKF model. RBFNN, radial basis function neural network; UKF, unscented Kalman filter [Colour figure can be viewed at wileyonlinelibrary.com]

RBFNN-UKF model and true SOC value is much smaller than that between the SOC estimated by the original RBFNN-UKF model and true SOC value in the presence of current sensor bias. Moreover, the extended RBFNN-UKF model can track the trueSOC value with high accuracy and fast speed while maintaining accurate and quick estimation for the current sensor bias. Validation for this conclusion can be seen from Figure 12.

4.3 | Discussion on the limitations

Both the proposed direct and indirect structures for SOC evaluation are based on NARX-NN and RBFNN-UKF, respectively. However, some limitations about the proposed models require to be discussed here. The discussion pointed out here can provide directions for future research work for SOC estimation.

1. Since the sampled data is derived from the charging and discharging experiment on brand-new lithium-ion batteries, the proposed direct and indirect estimators may not be applicable to the aging batteries. To this end, an approach that recording the sampled data through the lifetime of the battery can be employed to address this problem. A large memory, however, is required to store the data. Moreover, the accuracy of established NN models can be affected by the sampled data, consequently, it is necessary to guarantee the accuracy of the training data for the network.
2. For the established direct NARX-NN model, some initially unknown parameters such as the input and output time-delay order are all determined through trial and error experience. No scientific calculation methods have been developed to guide the determination of these parameters to extract the most accurate model. Similarly, the improvement for the RBFNN model accuracy can be considered in the further work.
3. Although the proposed extended RBFNN-UKF model realizes the simultaneous estimation of SOC and the current sensor bias, observability on the proposed extended RBFNN-UKF model has not been analyzed.
4. Charging and discharging experiment carried out on the battery and data collection are all based on the static experiment. On account of the difficulties in hardware realization and the limitations on measuring the negative current in real time by the sensors, the proposed SOC estimators have not been applied to the EVs for real-time monitor and analysis. Moreover, the disturbance to the battery is neglected.

5 | CONCLUSION

Direct and indirect NN-based structures for the battery SOC evaluation are proposed, trained, and compared in this article. Experimental results indicate that the direct NARX-NN estimator can realize effective and precise SOC estimation and has good robustness against different initial conditions. In addition, the indirect estimator based on RBFNN deems SOC as an internal state and, instead, voltage as the model output. UKF is utilized to estimate SOC based on the voltage error between the NN outputs and real measurements. For the regular estimation tasks, both estimators achieve similar overall accuracy, although the transient convergence of the direct NARX-NN is quicker than that of the indirect RBFNN-UKF estimator. However, the direct NARX-NN estimator deteriorated remarkably in the presence of current sensor bias. To remedy, the indirect RBFNN-UKF estimator can be readily modified by augmenting the current sensor bias as a new internal state variable which would be estimated together with SOC. In this regard, the indirect RBFNN-UKF estimator shows overwhelming superiority over the direct method. Experimental results prove the efficacy of the proposed estimators and depict a promising prospect in the future onboard applications.

ACKNOWLEDGEMENTS

This work was supported by National Natural Science Foundation of China under Grant 51806034 and 51936003, the Natural Science Foundation of Jiangsu Province, China under Grant BK20170686 and the open funding of the state key lab for engine, Tianjin University.

ORCID

Li Sun https://orcid.org/0000-0001-8960-8773

REFERENCES

1. Zubi G, Dufo-López R, Carvalho M, Pasaoglu G. The lithium-ion battery: state of the art and future perspectives. *Renew Sustain Energy Rev*. 2018;89:292-308.
2. Saw LH, Ye Y, Tay AAO. Integration issues of lithium-ion battery into electric vehicles battery pack. *J Clean Prod*. 2016;113:1032-1045.
3. Nykvist B, Nilsson M. Rapidly falling costs of battery packs for electric vehicles. *Nature Climate Change*. 2015;5(4):329-332.
4. Severson KA, Attia PM, Jin N, et al. Data-driven prediction of battery cycle life before capacity degradation. *Nat Energy*. 2019;4(5):383-391.
5. Hannan MA, Lipu MSH, Hussain A, Mohamed A. A review of lithium-ion battery state of charge estimation and management system in electric vehicle applications: challenges and recommendations. *Renew Sustain Energy Rev*. 2017;78:834-854.
6. Berecibar M, Gandiaga I, Villarreal I, Omar N, van Mierlo J, van den Bossche P. Critical review of state of health estimation methods of Li-ion batteries for real applications. *Renew Sustain Energy Rev*. 2016;56:572-587.
7. Jiang ZY, Qu ZG. Lithium-ion battery thermal management using heat pipe and phase change material during discharge–charge cycle: a comprehensive numerical study. *Appl Energy*. 2019;242:378-392.
8. Hu Y, Yurkovich S. Battery cell state-of-charge estimation using linear parameter varying system techniques. *J Power Sources*. 2012;198:338-350.
9. Huang D, Chen Z, Zheng C, Li H. A model-based state-of-charge estimation method for series-connected lithium-ion battery pack considering fast-varying cell temperature. *Energy*. 2019;185:847-861.
10. Pastor-Fernández C, Yu TF, Widanage WD, Marco J. Critical review of non-invasive diagnosis techniques for quantification of degradation modes in lithium-ion batteries. *Renew Sustain Energy Rev*. 2019;109:138-159.
11. Antón JCÁ, Nieto PJG, de Cos Juez FJ, et al. Battery state-of-charge estimator using the MARS technique. *IEEE Trans Power Electron*. 2012;28(8):3798-3805.
12. Piller S, Perrin M, Jossen A. Methods for state-of-charge determination and their applications. *J Power Sources*. 2001;96(1):113-120.
13. Kutluay K, Cadirci Y, Ozkazanc YS, Cadirci I. A new online state-of-charge estimation and monitoring system for sealed lead-acid batteries in telecommunication power supplies. *IEEE Trans Ind Electron*. 2005;52(5):1315-1327.
14. Zhang Y, Song W, Lin S, Feng Z. A novel model of the initial state of charge estimation for LiFePO4 batteries. *J Power Sources*. 2014;248:1028-1033.
15. Zheng L, Zhang L, Zhu J, Wang G, Jiang J. Co-estimation of state-of-charge, capacity and resistance for lithium-ion batteries based on a high-fidelity electrochemical model. *Appl Energy*. 2016;180:424-434.
16. Snihir I, Rey W, Verbitskiy E, Belfadhel-Ayeb A, Notten PHL. Battery open-circuit voltage estimation by a method of statistical analysis. *J Power Sources*. 2006;159(2):1484-1487.
17. Waag W, Sauer DU. Adaptive estimation of the electromotive force of the lithium-ion battery after current interruption for an accurate state-of-charge and capacity determination. *Appl Energy*. 2013;111:416-427.
18. Ma PY, Hu YB, Zhang XR. Research on adaptive power control parameter of a cold milling machine. *Simulat Modeling Pract Theory*. 2008;16(9):1136-1144.
19. Pozna C, Precup RE, Tar JK, Škrjanc I, Preitl S. New results in modelling derived from Bayesian filtering. *Knowledge-Based Syst*. 2010;23(2):182-194.
20. Gil A, Johanyák ZC, Kovács T. Surrogate model based optimization of traffic lights cycles and green period ratios using microscopic simulation and fuzzy rule interpolation. *Int J Artif Intel*. 2018;16(1):20-40.
21. Albu A, Precup RE, Teban TA. Results and challenges of artificial neural networks used for decision-making in medical applications, Facta Universitatis. *Mech Eng*. 2019;17(4):285-308.
22. Zhang CW, Chen SR, Gao HB, Xu KJ, Yang MY. State of charge estimation of power battery using improved Back propagation neural network. *Batteries*. 2018;4(4):69.
23. Shen Y. Adaptive online state-of-charge determination based on neuro-controller and neural network. *Energ Conver Manage*. 2010;51(5):1093-1098.
24. Charkhgard M, Farrokhi M. State-of-charge estimation for lithium-ion batteries using neural networks and EKF. *IEEE Trans Ind Electron*. 2010;57(12):4178-4187.
25. Liang MD, Wu TZ. An improved prediction method of SOC based on the GA-RBF neural network. *Adv Mater Res*. 2014;953:800-805.
26. Yan W, Zhang B, Zhao G, et al. A battery management system with a Lebesgue-sampling-based extended Kalman filter. *IEEE Trans Ind Electron*. 2018;66(4):3227-3236.
27. Sturm J, Ennifar H, Erhard SV, Rheinfeld A, Kosch S, Jossen A. State estimation of lithium-ion cells using a physicochemical model based extended Kalman filter. *Appl Energy*. 2018;223:103-123.
28. Wang T, Chen S, Ren H, Zhao Y. Model-based unscented Kalman filter observer design for lithium-ion battery state of charge estimation. *Int J Energy Res*. 2018;42(4):1603-1614.
29. Wang W, Wang X, Xiang C, Wei C, Zhao Y. Unscented kalman filter-based battery SOC estimation and peak power prediction method for power distribution of hybrid electric vehicles. *IEEE Access*. 2018;6:35957-35965.
30. Chen J, Ouyang Q, Xu C, et al. Neural network-based state of charge observer design for lithium-ion batteries. *IEEE Trans Control Syst Technol*. 2017;26(1):313-320.
31. Zhao S, Duncan SR, Howey DA. Observability analysis and state estimation of lithium-ion batteries in the presence of sensor biases. *IEEE Trans Control Syst Technol*. 2016;25(1):326-333.
32. He W, Williard N, Chen C, Pecht M. State of charge estimation for electric vehicle batteries using unscented kalman filtering. *Microelectron Reliab*. 2013;53(6):840-847.
33. Sbarufatti C, Corbetta M, Giglio M, Cadini F. Adaptive prognosis of lithium-ion batteries based on the combination of particle filters and radial basis function neural networks. *J Power Sources*. 2017;344:128-140.

34. Sun L, Hua Q, Shen J, Xue Y, Li D, Lee KY. Multi-objective optimization for advanced superheater steam temperature control in a 300 MW power plant. *Appl Energy*. 2017;208:592-606.
35. Sun L, Shen J, Hua Q, Lee KY. Data-driven oxygen excess ratio control for proton exchange membrane fuel cell. *Appl Energy*. 2018;231:866-875.
36. Sun L, Li G, Hua QS, Jin Y. A hybrid paradigm combining model-based and data-driven methods for fuel cell stack cooling control. *Renew Energy*. 2020;147:1642-1652.
37. Plett GL. Extended Kalman filtering for battery management systems of LiPB-based HEV battery packs: part 3. *State Parameter Estim J Power Sources*. 2004;134(2):277-292.
38. Vemuri AT. Sensor bias fault diagnosis in a class of nonlinear systems. *IEEE Trans Autom Control*. 2001;46(6):949-954.

SUPPORTING INFORMATION

Additional supporting information may be found online in the Supporting Information section at the end of this article.

How to cite this article: Sun W, Qiu Y, Sun L, Hua Q. Neural network-based learning and estimation of battery state-of-charge: A comparison study between direct and indirect methodology. *Int J Energy Res*. 2020;1–13. https://doi.org/10.1002/er.5654